Since January 2020 Elsevier has created a COVID-19 resource centre with free information in English and Mandarin on the novel coronavirus COVID-19. The COVID-19 resource centre is hosted on Elsevier Connect, the company's public news and information website.

Biosensors and Bioelectronics 192 (2021) 113550

Contents lists available at ScienceDirect

Biosensors and Bioelectronics

journal homepage: www.elsevier.com/locate/bios

Track-etched membrane microplate and smartphone immunosensing for SARS-CoV-2 neutralizing antibody

Cong Wang [a,1], Ze Wu [a,1], Bochao Liu [a,b,d,1], Panli Zhang [a,1], Jinhui Lu [a], Jinfeng Li [c], Peng Zou [a], Tingting Li [a], Yongshui Fu [d], Ruiai Chen [e], Ling Zhang [a,**], Qiangqiang Fu [f,***], Chengyao Li [a,*]

[a] Department of Transfusion Medicine, School of Laboratory Medicine and Biotechnology, Southern Medical University, Guangzhou, China
[b] Guangzhou Bai Rui Kang (BRK) Biological Science and Technology Limited Company, Guangzhou, China
[c] Shenzhen Key Laboratory of Molecular Epidemiology, Shenzhen Center for Disease Control and Prevention, Shenzhen, China
[d] Guangzhou Blood Center, Guangzhou, China
[e] Zhaoqing Branch Center of Guangdong Laboratory for Lingnan Modern Agricultural Science and Technology, Zhaoqing, China
[f] Department of Laboratory Medicine, Nanfang Hospital, Southern Medical University, Guangzhou, China

ARTICLE INFO

Keywords:
COVID-19 patients
Vaccinees
Neutralizing antibody
Track-etched membrane
Optical fiber
Smartphone

ABSTRACT

The level of neutralizing antibody (NAb) to SARS-CoV-2 could be used to evaluate the acquired protective immunity of COVID-19 patients or vaccinees. Here we develop a track-etched microporous membrane filtration microplate (TEM) and optical fibers transmitted immunosensing smartphone platform (TEMFIS) based surrogate virus neutralization test (TEMFIS-sVNT) for rapid one-step testing of NAb to SARS-CoV-2. Coefficient variation (CV) of intra-assay and inter-assay precisions of TEMFIS-sVNT varied below 9% or 14%, respectively. By agreement with pseudovirus neutralization test (pVNT) and ELISA-sVNT for testing of serum samples from 41 COVID-19 patients, 50 COVID-19 vaccinees and 320 healthy blood donors ($P = 0.895$), TEMFIS-sVNT detected the NAb positivity (sensitivity) in 92.68% COVID-19 patients and 76% vaccinees, but the NAb negativity (specificity) in 100% blood donors. In conclusion, TEMFIS-sVNT can be used for quantitatively point-of-care testing of neutralizing antibody to SARS-CoV-2 in blood samples from COVID-19 patients and vaccinees.

1. Introduction

The novel severe acute respiratory syndrome coronavirus 2 (SARS-CoV-2) has caused pneumonia disease since 2019 (COVID-19)(Q. Li et al., 2020), which has become a global pandemic. By the end of May 2021, more than 160 million people were infected with SARS-CoV-2 and over 3 million people were died. SARS-CoV-2 has a single strand positive RNA genome with length of ~29.8 kb (Gorbalenya et al., 2020; Chen et al., 2020; Wu et al., 2020; Ren et al., 2020), of which one third of genome encodes four structural proteins of spike (S), small envelope (E), matrix (M) and nucleocapsid (N)(Chan et al., 2020). S protein has a receptor-binding domain (RBD) that binds to viral receptor of human angiotensin-converting enzyme 2 protein (ACE2) mediating virus entry to the cells as well as induces neutralizing antibody (NAb) in the humans (Li and Fang, 2016; Zhou et al., 2020; Lan et al., 2020). Consequentially, SARS-CoV-2 RBD is used as a target for development of vaccines or therapeutic NAb against COVID-19 (Lan et al., 2020; Luo et al., 2019, 2020, 2021).

Detection of NAb to SARS-CoV-2 can help to evaluate the acquired protective immunity in COVID-19 patients and vaccines (Zhou et al., 2019; Barnes et al., 2020). However, current NAb assays are mostly time-consuming on cell culture and not suitable for rapidly clinical assessment. Due to live virus operation, the conventional virus neutralization test (cVNT) for SARS-CoV-2 is restricted under biosafety level 3 (BSL-3) facilities (Mendoza et al., 2020), while the pseudovirus-based VNT (pVNT) also requires cell culturing under biosafety level 2 (BSL-2) facilities (Hu et al., 2020; Nie et al., 2020). Recently, an enzyme immunoassay (EIA) with antibody-mediated blockage of the interaction between RBD and ACE2 was established for the surrogate virus neutralization test (sVNT) without cell operation

* Corresponding author.
** Corresponding author.
*** Corresponding author.
E-mail addresses: zhangling1982@163.com (L. Zhang), 982623065@qq.com (Q. Fu), chengyaoli@hotmail.com (C. Li).
[1] These authors contributed equally to this work.

https://doi.org/10.1016/j.bios.2021.113550
Received 21 June 2021; Received in revised form 26 July 2021; Accepted 4 August 2021
Available online 8 August 2021

(Tan et al., 2020; Abe et al., 2020; Walls et al., 2020), of which here it was refereed as ELISA-sVNT. In clinical practice, to advance sVNT, a rapid and easy performing assay is deserved urgently for quantitatively point of care testing (POCT) of NAb among COVID-19 patients or vaccinees.

In this study, we designed a track-etched membrane (TEM) filtration microplate and optical fibers transmitted portable immunosensing smartphone reader platform (TEMFIS) based surrogate virus neutralization test (TEMFIS-sVNT) for one-step point of care testing of NAb to SARS-CoV-2. In comparison with pVNT and ELISA-sVNT, the established TEMFIS-sVNT was evaluated by detecting clinical blood samples from COVID-19 patients and vaccinees.

2. Materials and methods

2.1. Blood specimens

A number of 41 convalescent serum samples of COVID-19 patients were provided by the Shenzhen Center for Disease Control and Prevention (CDC), China. Totally 50 COVID-19, 8 rabies, 8 hepatitis B, 6 human papilloma vaccinees' serum samples and 6 COVID-19 vaccinees' whole blood samples were collected at the Southern Medical University Nanfang Hospital, China. A total of 323 plasma samples and 4 whole blood samples of none SARS-CoV-2 infected or COVID-19-vaccinated healthy blood donors were collected as negative controls from the Chinese Blood Centers in Guangzhou (South), Harbin (Northeast), Chengdu (Southwest) and Xi'an (Northwest) cities of China. All COVID-19 patients' serum samples were inactivated for 40 min by heating at 56 °C in the water bath.

The use of human blood samples in the study was approved by Southern Medical University Medical Ethics Committee, and followed the ethical guidelines of the 1975 Declaration of Helsinki.

2.2. Chemicals and equipment

Polystyrene microbeads COOH- (PBs, 5, 10 and 26 μm particles in size) were purchased from Tianjin Saierqun Technology Co. Ltd (Tianjin, China). N-hydroxy-succinimide (NHS) and 1-(3-Dimethylaminopropyl)-3-ethylcarbodiimide hydrochloride (EDC) were purchased from BBI Life Science (Shanghai, China). 2-(N-Morpholino)ethanesulfonic acid monohydrate (MES) was purchased from Shanghai Macklin Biochemical Co., Ltd (Shanghai, China). Tween-20, bovine serum albumin (BSA) and 3,3′,5,5′– tetramethylbenzidine (TMB) were purchased from Sigma (St. Louis, USA). Track-etched polycarbonate microporous membranes (TEM, three pore sizes of 1, 3 and 5 μm) were purchased from Beijing Tsingneng Chuangxin Science and Technology Co., Ltd (Beijing, China). Electroluminescence panel (EL, 450 nm) was purchased from Xinlong Lightwear (Shenzhen, China). The polymethyl methacry late (PMMA) optical fibers with 1.5 mm diameter were purchased from Shenzhen Chuangli Fiber Optic Material Co., Ltd. (Shenzhen, China). Opaque photosensitive resin was purchased from Novartis Intelligent Technology Co., Ltd. Fc-RBD and ACE2 proteins (for TEMFIS-sVNT) were purchased from ACRO Biosystems (Beijing, China). Activated HRP labeling kit purchased from StarBio (Jinan, China). Mouse monoclonal antibody (1F2-2) to RBD of SARS-CoV-2 was provided in this laboratory. His-RBD and ACE2 proteins (for ELISA-sVNT), HEK-293T and HEK293T-hACE2 cells were purchased from Sino Biological (Beijing, China). Goat anti-mouse his-tag HRP conjugates were purchased from Biolab Technology Co. Ltd (Beijing, China). PsPAX2 and plasmid pLenti-CMV Puro-Luc were purchased from Addgene (USA). The plasmid pcDNA3.1-SARS-CoV-2SΔCT (the cytoplasmic tail deleted) was prepared in the laboratory. Steady-Glo Luciferase Assay was purchased from Promega (Wisconsin, USA).

2.3. Preparations of ACE2-labeled PBs and RBD-conjugated HRP

The amounts of 60 μl of PBs (250 mg/ml) were washed with 100 μl of 50 mM MES (pH 4.9) and re-suspended in 200 μl MES after 3min and 10,000g centrifugation. The volumes of 2.5 μl EDC (1 mg/ml) and 2.5 μl NHS (2 mg/ml) were added to PBs and incubated for 30 min at room temperature. The excessive EDC and NHS were removed by centrifugation. The amounts of 30 μg ACE2 were added to the activated PBs and incubated for 3 h at room temperature. Taking 200 μl of 2% BSA were added to block PBs' spare surface for 1 h and the supernatant was removed by centrifugation. Finally, ACE2-PBs were resuspended in 300 μl preservation solution (1% BSA, 10% trehalose, 5% sucrose, 10 mm Tris HCl buffer, pH 8.0), stored at 4 °C. RBD-HRP conjugates were prepared by mixing the activated HRP and Fc-RBD in 1:2 ratio, adjusting the pH to 9.5 and then incubating at 37 °C for 1 h. Finally, the reaction solution was adjusted to pH 7.0 for storage after adding 2 mg sodium borohydride.

2.4. Pseudovirus neutralization test (pVNT)

The plasmid DNAs of pcDNA3.1-SARS-CoV-2 SΔCT, psPAX2 and pLenti-CMV Puro-Luc were co-transfected into HEK-293T cells for 48 h. The pseudoviruses carrying SARS-CoV-S were collected from the supernatants of cell cultures by filtration through 0.45 μm filter. HEK293T-hACE2 cells were seeded in 96-microwell plates at 4×10^4 cells/well. Taking 50 μl of pseudoviruses were incubated with two-fold serially diluted serum (initiating at 1:10) samples for 60 min at 37 °C. The mixtures were then laid onto HEK293T-hACE2 cell in microwell plates. Cells were lysed and tested by Steady-Glo Luciferase Assay. Viral titers were determined 48 h post-infection. Inhibition (%) = (1 − sample RLU/control RLU) × 100. Log10 pVNT (ID_{50}) titer was reported.

2.5. Fabrication of TEM-microplate

The 76 × 76 mm microplates with 64 un-bottomed wells (8 × 8 array; 12 mm in diameter each well) were fabricated by photocuring 3D printing using opaque photosensitive resin materials. The double-side adhesive was pasted on the bottom of microplate and the 64-wells were re-generated by a punch. Three types of TEMs (5 μm thick) with 1, 3 and 5 μm pores were selected for soaking in 2% BSA solution for 2 h, and then dried and sealed on the bottom adhesive of microplate (TEM-microplate). To determine proper pore size of TEM for liquid retention and filtration rates, 100 μl of 1: 20 diluted serum or whole blood were added into microwells for standing 30 min, and then placed on absorbent papers for filtration at room temperature. The liquid volume inside the wells was measured after standing of 30 min, and the time for liquid filtration was calculated. The TEM with optimal pore size showing the full liquid retention during standing and the faster percolation during absorption was selected.

2.6. A platform of electroluminescence immunosensing through optical fiber transmission smartphone reader

A handheld smartphone reader in-stored with an app was designed for sensing electroluminescence (EL) signals through the catalyzed substrate filtration in 64-well TEM-microplate and individual optical fiber transmissions. This device consists of an 80 × 80 mm EL panel on the box cover, 64-microwell TEM-microplate, 64-microwell isolator-board (2 mm thick), base-board with 64 individual optical fibers (a diameter of 1.1 PMMA each), smartphone holder, app in-stored smartphone, switch and USB-interface on the side of box. An EL panel emits 450 nm blue light. The 64 optical fibers (up to 160 mm length) gather to an 8 × 8 array in a small square hood on right-top corner facing smartphone camera. The isolator and base boards, smartphone holder and box were fabricated by photocuring 3D printing with opaque photosensitive resins.

2.7. Detection of NAb by TEMFIS-sVNT

Serum or whole blood samples (an initial dilution with 1:10) were 2-folds serially diluted to 1:1280. The mixture of 50 μl of dilution sample and 50 μl of RBD-HRP conjugates was added in TEM-sealed microplate, and followed by adding 5 μl ACE2-PBs for 30 min at room temperature. After washing the microplate once on absorbent papers by filtration with 0.05% Tween-20 PBS, 100 μl of TMB substrate solution were added for reacting for 15 min, then stopped by adding 50 μl of 2M H_2SO_4 for terminating reaction. The microplate was properly mounted in the TEMFIS device, and the blue light of EL emission was filtrated through color-changed substrates in TEM-microwells and were transmitted via 64 optical fibers to an app in stored smartphone reader, where the light images were captured and the light intensities were converted to gray-scale values (GS) for reporting results. Grayscale value (GS) = (Intensity value of blank - Intensity value of test)/Intensity value of test. The following formula is used to calculate NAb activity, of which a cutoff at equal or more than (≥) 30% inhibition rate is considered positive according to a previous evaluation on NAb efficacy (CI = 14.4–28.4%) (Khoury et al., 2021). Inhibition rate (%) = (1 − sample GS/negative control GS) × 100. The pVNT and ELISA-sVNT were used as control assays for measuring NAb to SARS-CoV-2 (Nie et al., 2020; Tan et al.,

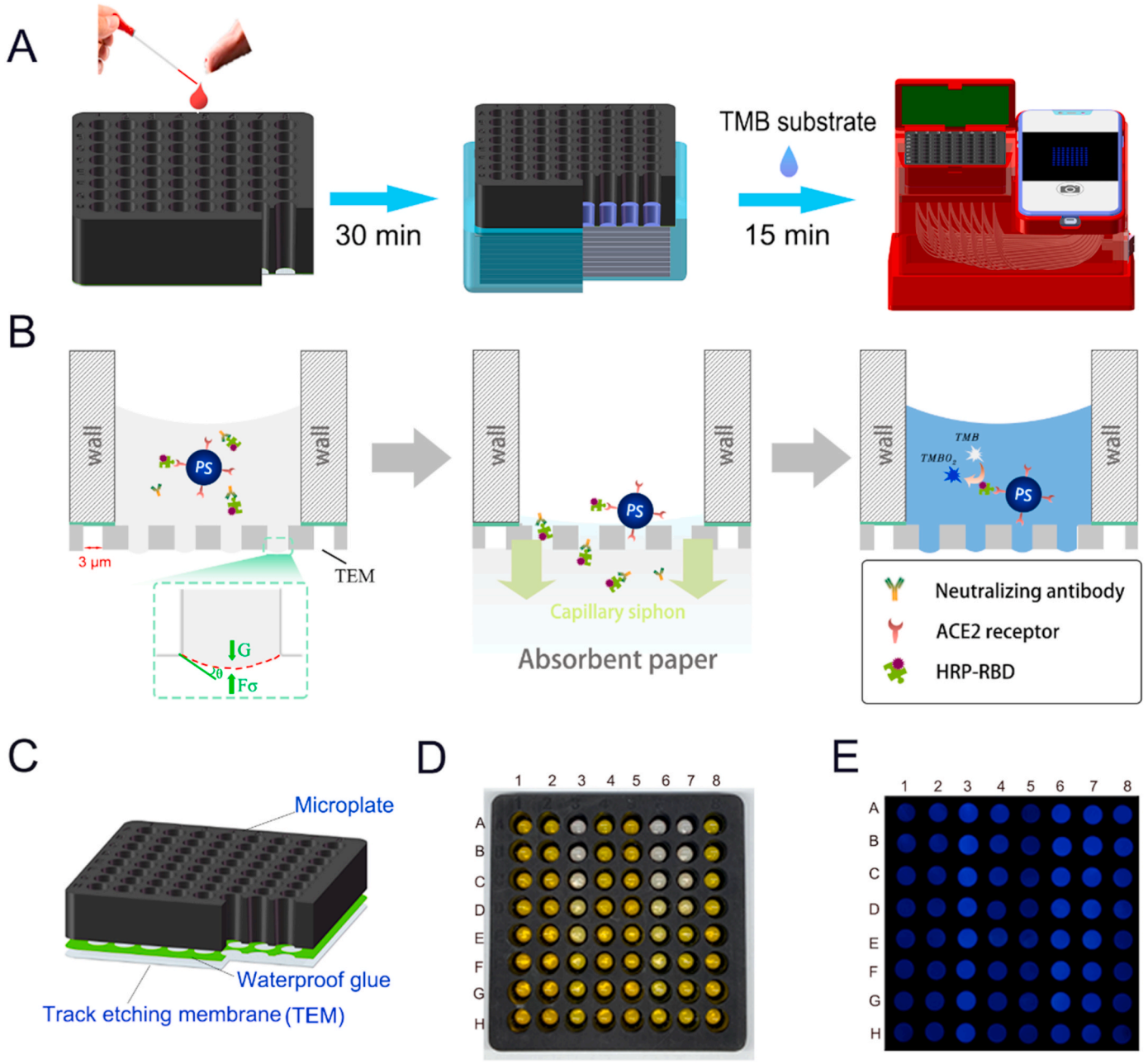

Fig. 1. Operation diagram and principle of TEMFIS-sVNT. (A) Operation procedure of TEMFIS-sVNT. The mixture of diluted serum sample and RBD-HRP solution is added into TEM-microplate to incubate for 30min (left panel), then the TEM-microplate is washed once by absorbent papers (central panel). TMB substrate solution is added into TEM-microplate to react for 15 min and then terminated by 2M H_2SO_4. Finally, the reactive plate is mounted into the TEMFIS device for detection and analysis (right panel). (B) Principle of sVNT in TEM microplate. (C) The structure of a representative 64-well TEM-microplate with an 8 × 8 microwell array, waterproof glue and TEM. (D) A representative of photographic colors of catalyzed substrates corresponding to individual samples in TEM-microplate. (E) The images of blue EL lights are captured through substrate filtrations and individual optical fiber transmissions by a smartphone reader and camera. (For interpretation of the references to color in this figure legend, the reader is referred to the Web version of this article.)

2020).

2.8. Statistical analysis

GraphPad Prism 8.0 is used for correlation analysis. The data are represented as the means ± SD from three independent experiments. The *P* values are calculated by the paired and unpaired two-tailed Student's t-tests, of which P value < 0.05 is considered statistically significant. The difference in detection sensitivity among three assays was calculated by Pearson's chi-squared test using the statistical package SPSS v. 16.0.

3. Results

3.1. Principle of TEMFIS-sVNT for one-step quantification of SARS-CoV-2 NAb

TEMFIS-sVNT is principally based on one-step surrogate virus neutralization test (sVNT) for measuring of protective antibody to SARS-CoV-2 in TEM-microplate with optical fibers transmission immunosensing smartphone reader platform (TEMFIS) (Fig. 1A). In this assay, sVNT is to measure sample's NAb competitive binding to RBD-HRP conjugates and further to block RBD-HRP conjugates binding to ACE2-PBs in TEM-microplate (Fig. 1B). One-step detection benefits from 64-well TEM-microplate (Fig. 1C). The reacting liquids retain in the wells due to the liquid's surface tension and form tiny liquid protrusion at the bottom of TEM-microplate (Fig. 1B, left and right panels), while when liquid protrusions of TEM contact with absorbent papers, the liquids (NAb-RBD-HRP/RBD-HRP) are washed away by filtration with the 3 μm pore size TEM under capillary siphoning and the 5 μm ACE2-PBs or ACE2-PBs-RBD-HRP complexes are retained in TEM-microplate (Fig. 1B, central panel). After adding TMB substrate in TEM-microplate, the reaction presents weak yellow or no color change, implying NAb positive to RBD, while inversely TMB substrate becomes strong yellow, suggesting NAb negative to RBD (Fig. 1D). For reporting the color changes of substrates, the blue EL panel emission (450 nm) is applied to pass through the catalyzed substrates (from no color to strong yellow) in 64-well TEM-microwells. The substrate-filtered blue lights are transmitted through 64 individual optical fibers to an app in-stored smartphone reader, where the images of light intensities at 8 × 8 array are captured by corresponding to individual microwells (Fig. 1E). The intensities of blue EL signals are calculated by smartphone app, of which the strong light indicates presence of NAb in serum samples, while the weak or no light suggests absence of NAb in testing samples. By converting of light intensities to GS values and correlating with inhibition rates by an in-stored app, the NAb levels are reported for individual blood samples.

3.2. Design of TEM-microplate and TEMFIS

The photocuring 3D printed 64-well microplate with TEM sealed bottom (Fig. S1A) was designed for one-step sVNT for detecting NAb from blood samples. TEM is characterized by accurate pore size, fast flow rate and excellent chemical corrosion resistance. To maximize the retention of liquids in TEM-microwells during incubation for 30 min at room temperature, or to fasten liquid filtration and minimize the liquid residues in TEM-microplate during washing on the absorbent papers, 100 μl of serum or whole blood diluents were added to 1, 3 and 5 μm pore sizes of TEM-microplate. The TEM with 3 μm pore size and 5 μm thick was observed for 100% retention during incubating and 20 s complete filtration during washing, which was selected for use in TEMFIS-sVNT (Table S1). The TEM is transparent and can be penetrated by most lights (Fig. S1B). Scanning electron microscope (SEM) images demonstrate that 3 μm pores distributed throughout TEM (Fig. S1C), and the 5 μm PB were separated on the membrane when the reacting solution was filtered through the membrane (Fig. S1D). No liquid effusion was observed during incubating for 30 min (Fig. S1E), while no liquid residue was retained when filtration was applied (Fig. S1F). For testing of 64 samples, it takes 45 min and costs only $0.02 for a piece of TEM, while the microplate is re-useable. This 64-well TEM-microplate makes it possible for rapid and high-throughput detection in immunoassays.

3.3. Characterization of TEMFIS

A device for TEM-microplate and optical fiber transmission immunosensing smartphone reader platform (TEMFIS) has been designed for measuring of the color changes of TMB substrate reactions corresponding to the presence of NAb in individual samples (Fig. 2A). At inner side of TEM-microplate cover, EL panel powered by smartphone OTG mode emits the homogenized and none self-heated blue light (450 nm wavelength), which are through the reacted substrate filtrations and transmitted to an app in-stored smartphone reader via 64 individual optical fibers (Fig. 2A). Blue EL lights are captured by smartphone camera as images at a 8 × 8 array corresponding to 64 samples' reactions in TEM-microplate (Fig. 2B), which are extremely tighten by connecting with optical fibers within a largely reduced reader cubage (Fig. 2B). The information of array images are processed by an in-stored custom-designed app, in which the intensity of blue light in each well is converted as GS value, respectively. In this study, a strong correlation was observed between the smartphone calculated GS values and OD450 values ($R^2 = 0.9715$, $P < 0.0001$; Fig. 2C), suggesting that TEMFIS was a reliable POCT device for rapid diagnosis in clinical practice. The results are presented as NAb inhibition rate or clinical outcome (negativity or positivity) by calculating GS value versus negative control with an in-stored app of smartphone (Fig. 2D).

3.4. Data Processing via smartphone application

When sample reaction is finished, TEM-microplate is placed onto TEMFIS device (Figs. 1A and 2A). In the working flowchart of data processing, the blue EL emission passes through substrate filtrations and the blue lights are transmitted via optical fibers to smartphone reader, where the images with various light intensities in corresponding to individual sample wells are captured (Fig. 2B and D). To process these images, the custom application is in-stored in a smartphone (Fig. 3). From the main menu (Fig. 3A), the user can select a type of immunoassays from Project. When starting a new test, the operating interface appears to set the parameters of light wavelength and testing wells for measuring neutralizing antibody to SARS-CoV-2 (Fig. 3B). Once setting up, the project is submitted to take photo and then to select light intensity image map for analyzing the data (Fig. 3C). The light intensity map is converted to GS map (I) by an in-stored app of smartphone reader (Fig. 2D). To standardize the changes of light intensities from testing wells, a blank reference well is used as a background control of GS (I_0) (Fig. 2D). According to the custom-designed formula, sample's GS value is calculated as below:

$$GS\ value = (I_0 - I)/I.$$

Furthermore, NAb inhibition rate (%) is calculated as below basing on the GS value of each testing well against a negative control sample.

$$\%\ Inhibition = (1 - sample\ GS\ /\ control\ GS)*100.$$

For reporting clinical outcome, the qualitative (positive or negative) report can be released (Fig. 3D), while for analyzing NAb level, the quantitative (inhibition rate) report can be exported (Fig. 3E). In addition, the history record can be viewed, including the date and clinical information of testing samples (Fig. 3F).

3.5. Optimization of one-step TEMFIS-sVNT

By using TEM-microplate, the reacting conditions of one-step TEMFIS-sVNT were optimized for PBs size, RBD-HRP or ACE2-PBs concentration, and reaction time, respectively. The optimal parameters were

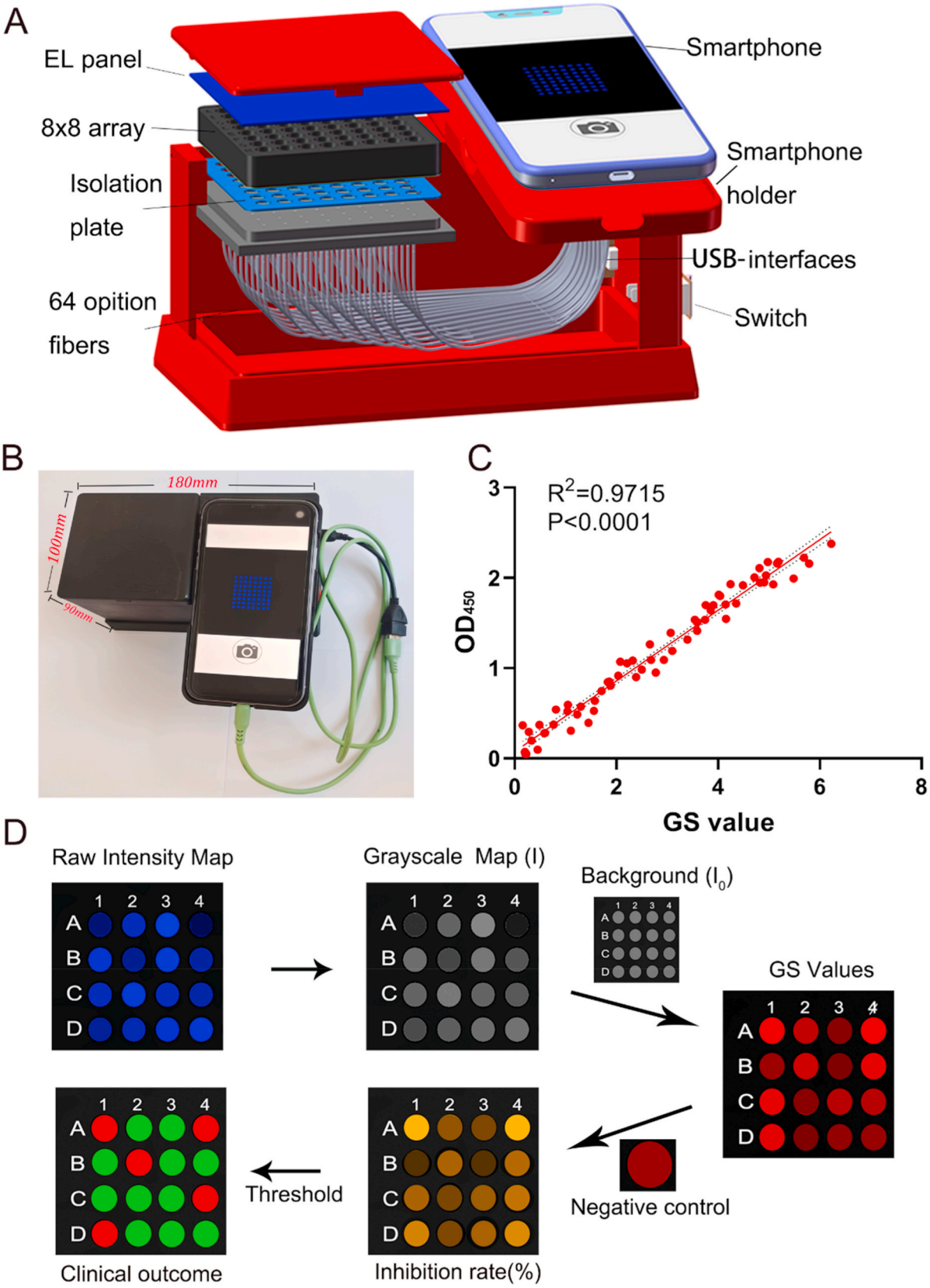

Fig. 2. TEMFIS device and working flowchart. (A) The device of TEMFIS. (B) A smartphone reader device. (C) Correlation of TEMFIS GS and ELISA OD_{450} values measured from 64-well microplate. (D) Flowchart of TEMFIS-sVNT for processing light signals and data. Firstly, the blue light intensities of images are converted to images of GS, divided by each well background and then GS values are calculated. Next, NAb inhibition (%) is obtained by using the formula (% Inhibition= (1−sample GS/control GS) *100). Finally, the inhibition (%) is presented to clinical outcomes (positivity or negativity) by a threshold inhibition rate such as 30%. Correlation is analyzed by GraphPad Prism. Data represents the mean ± Standard deviation (SD) of three replicates. (For interpretation of the references to color in this figure legend, the reader is referred to the Web version of this article.)

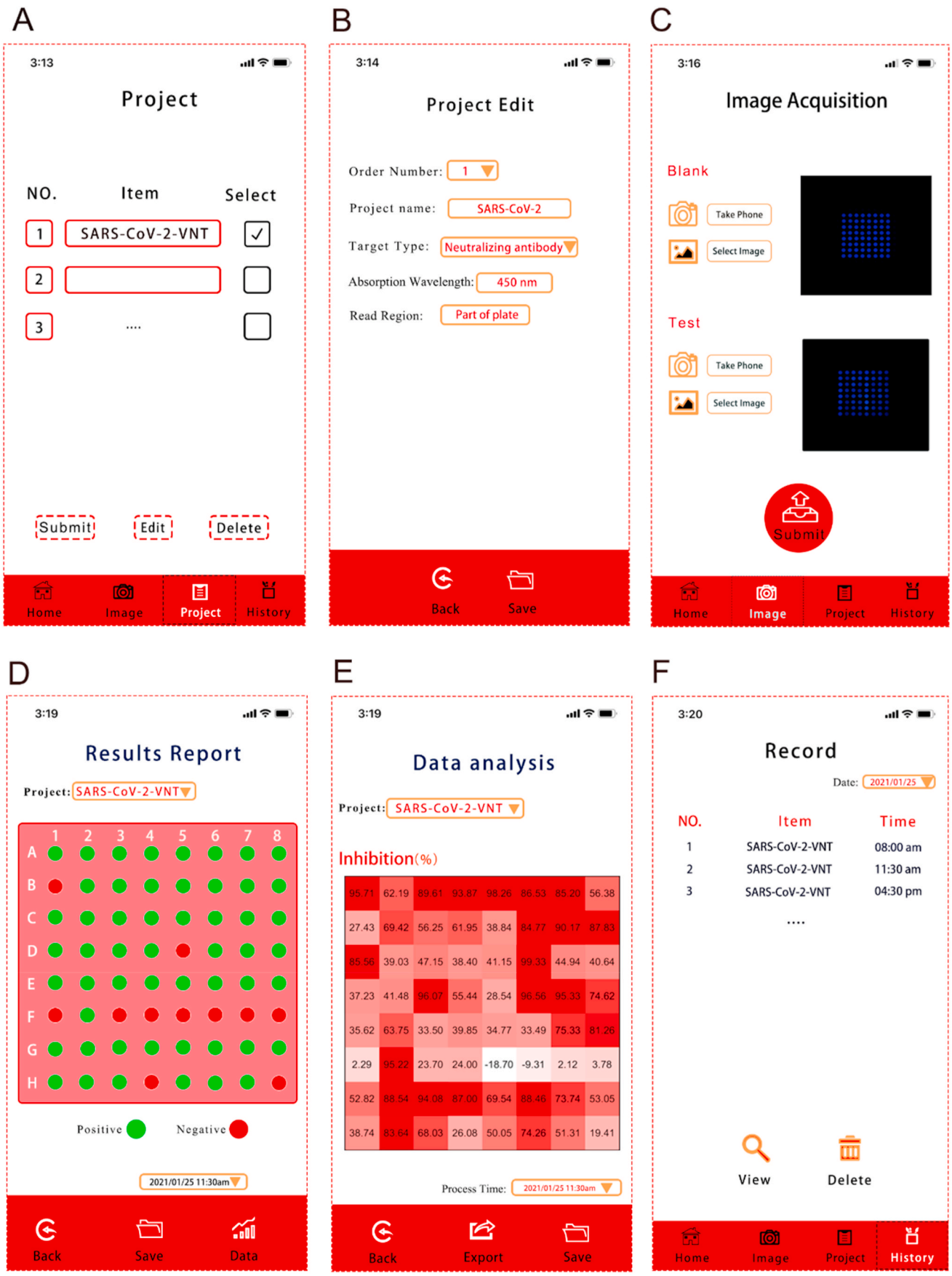

Fig. 3. Screenshots from the smartphone-based optic fiber reader app. (A) Select detection items. (B) Edit items (number, type of items, etc.). (C) Select images for data analysis. (D) Show qualitative results. (E) Quantitative results inhibition rate. (F) History record of detection item, time and sample submission.

modeled by the better reaction (GS or R^2 value) and the less concentration or time (Fig. 4). The sizes of 5, 10 and 26 μm PB (>3 μm pore size of TEM) were tested for conjugating with ACE2, of which the 5 μm PB-ACE2 conjugates showed the strongest reaction and selected for subsequent experiments (Fig. 4A). The volumes (50 μl) of 80, 160, 320, 640 and 1280 ng/ml RBD-HRP conjugates were cross-titrated with 2, 5, 10 and 15 μl ACE2-PBs/well, respectively (Fig. 4B), in which 5 μl ACE2-PBs/well were optimally selected to determine the concentration of RBD-HRP conjugates. By using a mouse monoclonal antibody (mAb1F2-2) to SARS-CoV-2 RBD, the concentration of RBD-HRP conjugates for 50% inhibiting deduction (ID_{50}) would be selected (Fig. 4C), in which 320 or 640 ng/ml RBD-HRP presented a linear correlation coefficient (R^2) greater than 0.98, and finally 320 ng/ml RBD-HRP conjugates were chosen for subsequent experiments. By selecting the appropriate reaction time, one-step TEMFIS-sVNT was performed for 10, 20, 30, 45, 60, 75 and 90 min incubations for reacting with the mixture of diluted

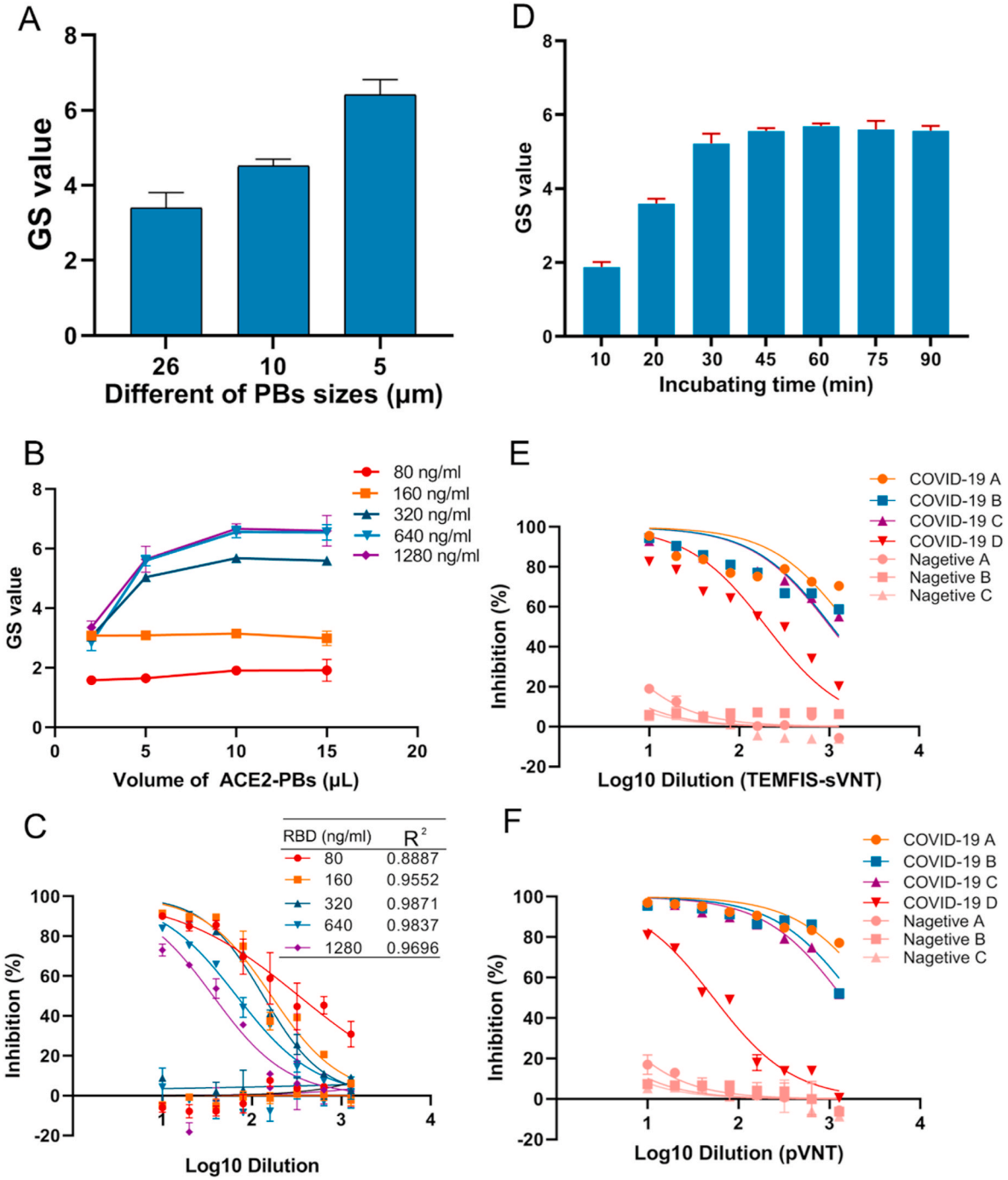

Fig. 4. Optimization of one-step TEMFIS-sVNT. A standard reaction of sVNT contains 50 μl of dilution sample, 50 μl of RBD-HRP and 5 μl of ACE2-PBs conjugates in TEM-microwell. (A) The reacting efficiency of ACE2-PBs conjugates with three different PBs sizes. (B) Different concentrations of RBD-HRP reacted with ACE2-PBs. (C) Determination of proper concentration of RBD-HRP on inhibition (%) corresponding to R^2 values. Inhibition of RBD-HRP interaction with ACE2-PBs was examined by a mouse monoclonal antibody to SARS-CoV-2 RBD (1F2-2). (D) Selection of optimal time for RBD-HRP and ACE2-PBs reaction. (E) Verification of one-step TEMFIS-sVNT by testing 4 COVID-19 patient serum samples and 3 negative controls. (F) Testing for NAb inhibition of COVID-19 patient serum samples and controls by pVNT. The data represents the mean ± SD of three replicates.

serum sample, RBD-HRP conjugates and ACE2-PBs in TEM-microplate, respectively. The GS values tended to be stable at 30 min incubation for reaction (Fig. 4D).

Further to verify the feasibility of one-step TEMFIS-sVNT under optimal conditions at 50 μl of diluted sample, 50 μl of 320 ng/ml RBD-HRP, 5 μl of ACE2-PBs, 30 min sample incubation and 15 min substrate reaction, a number of 4 convalescent sera of COVID-19 patients and 3 negative sera of blood donors were tested (Fig. 4E), in which 4 COVID-19 patients' serum samples presented NAb ID_{50} titers >100, while 3 blood donors' controls were NAb negative. These results were consistent with those detected by pVNT (Fig. 4F). Further to validate the specificity of one-step TEMFIS-sVNT in TEM-microplate, the serum samples from 8 rabies, 8 HBV and 6 HPV vaccinated individuals were examined (Fig. 5A), of which no cross-neutralizing antibody was detected.

Coefficient variations (CV) of intra- and inter-assays were evaluated for precision and accuracy of TEMFIS-sVNT by testing of high, middle and low activity of NAb from COVID-19 patients' serum samples at 1:20 dilution. Intra-assay CV varied below 9.0% among 16 replicates in TEM-microplate (Fig. 5B), while inter-assay CV ranged between 2.8% and 14.0% among 16 independent tests in TEM-microplates (Fig. 5C). The results indicated that the TEMFIS-sVNT had the higher stability and precision.

In addition, one-step TEMFIS-sVNT was also attempted for detecting whole blood samples. By adding 1:2.5–1:25 diluted whole blood in TEM-microplate, the red cells were not seen in the bottom of wells after absorbent filtration (Figure S2A, B and C). When 10 μl or less of whole blood samples were mixed with 100 μl of RBD-HRP and PBs-ACE2 solution/well for 30 min incubation in TEM-microplate, the background GS values of TEMFIS-sVNT were <1 (Fig. S2D). By using 5 μl of optimal volume of whole blood sample, 10 whole blood samples from 6 COVID-19 vaccinees and 4 unvaccinated blood donors were tested by TEMFIS-sVNT, in which 6 COVID-19 vaccinees presented 30–200 NAb ID_{50} titers, while 4 blood donors were NAb non-reactive (Fig. S2E).

3.6. Detection of NAb to SARS-CoV-2 in clinical samples by TEMFIS-sVNT

By using the established TEMFIS-sVNT, the NAb was measured in plasma samples from 41 COVID-19 patients and 40 vaccinees in comparison with ELISA-sVNT and pVNT, respectively. The levels of NAb to SARS-CoV-2 were presented as ID_{50} titers and were compared between these three assays (Table S2). The TEMFIS-sVNT NAb levels were significantly correlated with pVNT ($R^2 = 0.7856$, $P < 0.0001$; Fig. 6A) and ELISA-sVNT ($R^2 = 0.8816$, $P < 0.0001$; Fig. 6B), while pVNT and ELISA-sVNT ID_{50} titers were also correlated statistically ($R^2 = 0.8159$, $P < 0.0001$; Fig. 6C). The data suggested that TEMFIS-sVNT was a reliably rapid assay for quantitatively point of care testing of NAb to SARS-CoV-2 from COVID-19 patients or vaccinees.

To validate TEMFIS-sVNT performance in detection of clinical samples, 320 plasma samples from none SARS-CoV-2 infected or COVID-19 vaccinated healthy blood donors were tested. The inhibition rates of 320 donor plasmas at 1:20 dilution ranged between −7.79% and 13.4% (95% confidence interval; Fig. 6D). Consequently, a cutoff ≥30% inhibition rate was chosen as a line for determining NAb positive to SARS-CoV-2 in clinical outcome, in reverse the inhibition rate less than (<) 30% was NAb negative in blood samples (Fig. 6D). The NAb inhibition activity was detected from 92.68% (38/41) COVID-19 patients and 76% (38/50) COVID-19 vaccinees, respectively (Fig. 6D). Comparing three assays for detecting NAb to SARS-CoV-2 according to the cutoff of 30% inhibition, an overall of 83.52% sensitivity were found by TEMFIS-sVNT, which were consistent with pVNT and ELISA-sVNT ($P = 0.895$), while 100% specificity were observed for all three assays (Table S3).

4. Discussion

In this study, one-step TEMFIS-sVNT in TEM-microplate is principally based on the EIA based antibody interacting with ACE2 protein *in vitro* assay, modeling NAb blocks SARS-CoV-2 virus binding to human cell receptor *in vitro* or *in vivo* (Passariello et al., 2021; Shi et al., 2020). ELISA-sVNT has been previously reported for strongly correlating with both cVNT and pVNT (Tan et al., 2020), and does not require live virus and cell culture operation for NAb measurement. However, this ELISA-sVNT is operatively complicated and time-consuming, and it still relies on special equipment for reading substrate reactions in microplate, restricting its use in clinical practice. In contrast, one-step TEMFIS-sVNT was beneficial from TEM-microplate and simply finished within 45 min. TEM has the smooth surface and no adsorption of liquids, of which the precision filtration characteristics can be used to filter excessive reactants smaller than its pore size (Tian et al., 2020; Wang et al., 2012). Based on filtration with 3 μm pore size of TEM in this study, the blood components of more supple erythrocytes, smaller platelets and fresh plasma are allowed to pass or be washed away (Rodriguez et al., 2005; Jokerst et al., 2008), but 5 μm PB complexes are retained in the TEM-microwells. Therefore, one-step TEMFIS-sVNT with

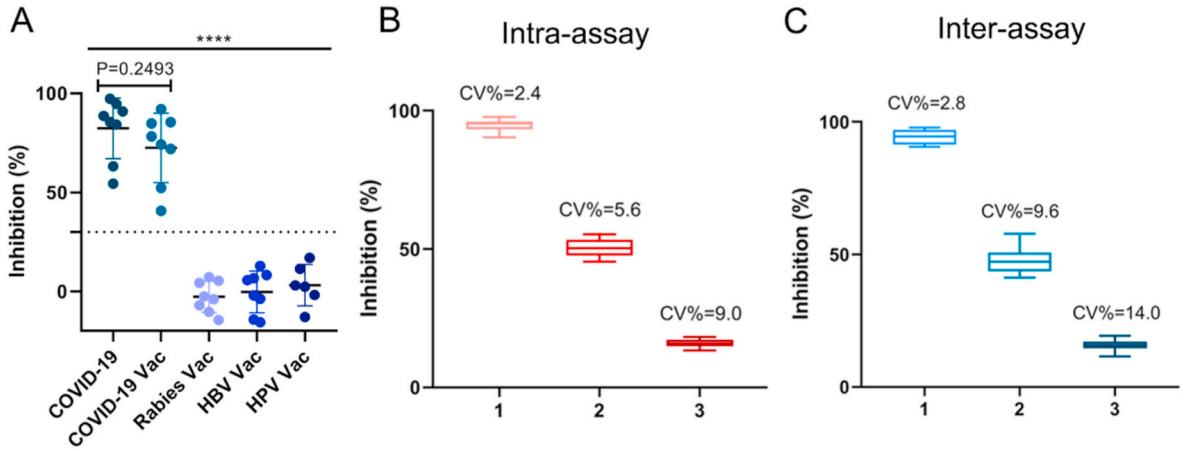

Fig. 5. Specificity and accuracy of TEMFIS-sVNT. (A) TEMFIS-sVNT was tested for the reactivity of serum samples from COVID-19 patients (n = 8) and vaccinees (Vac) of COVID-19 (n = 8), Rabies (n = 8), Hepatitis B (HB, n = 8) and Human papilloma (HP, n = 6). (B) Intra-assay CV of TEMFIS-sVNT for 16 replicates with high, middle or low activity of NAb from COVID-19 patients' serum samples (1:20 dilution). (C) Inter-assay CV of TEMFIS-sVNT for 16 independent tests with high, middle or low activity of NAb from COVID-19 patients' serum samples (1:20 dilution). Coefficient of variation (CV) = (SD/Mean) × 100%. Mean: Average inhibition rate at 1:20 dilution of COVID-19 serum samples was obtained from different time repetitions or batches. The dotted line indicates that the cutoff at 30% inhibition rate. The *P* values are calculated from unpaired and paired two-tailed Student's t-tests. The data represents the mean ± SD of three replicates. ****$P < 0.0001$.

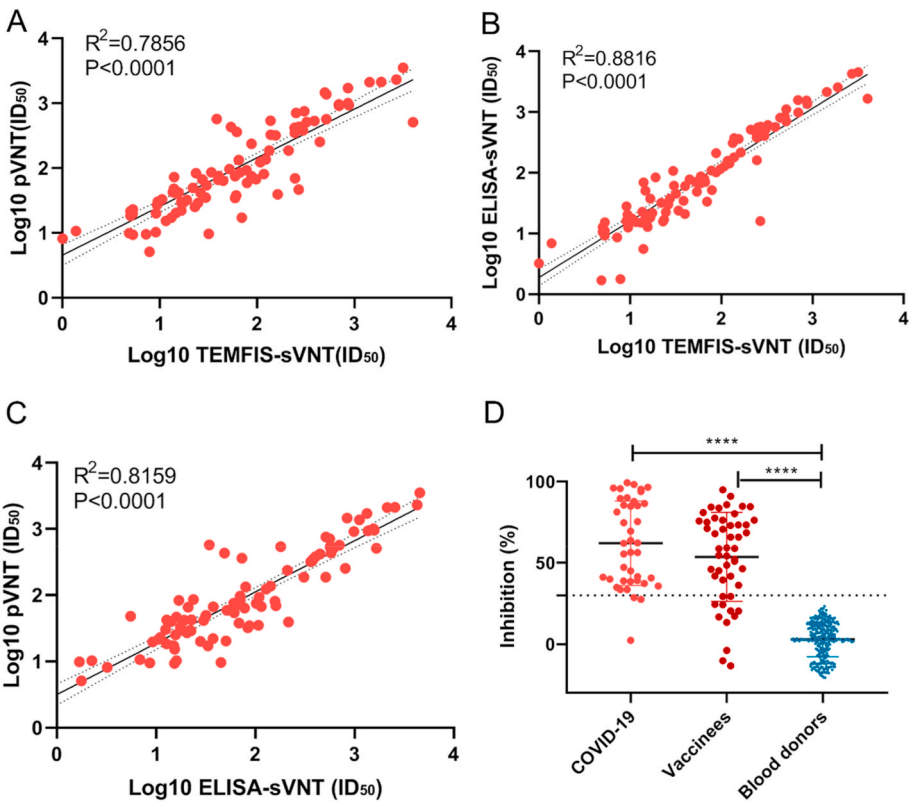

Fig. 6. TEMFIS-sVNT for detection of NAb in clinical samples. (A) Correlation between TEMFIS-sVNT and pVNT; (B) TEMFIS-sVNT and ELISA-sVNT; (C) pVNT and ELISA-sVNT for quantification of NAb in 41 COVID-19 patients and 50 vaccinees serum samples. (D) Quantification of NAb to SARS-CoV-2 in COVID-19 patients (n = 41), COVID-19 vaccinees (n = 50) and blood donors serum samples (n = 320) at 1:20 dilution by TEMFIS-sVNT. The dotted line indicates that the cutoff at 30% inhibition. The *P* values are calculated from unpaired and paired two-tailed Student's t-tests. Correlation is analyzed by GraphPad Prism. The data represents the mean ± SD of three replications. ****$P < 0.0001$.

TEM-microplate can be used to detect both serum/plasma and whole blood samples.

Currently, most optical imaging used in rapid diagnostic methods, such as a digital camera and a flatbed scanner, are to capture the entire plate information, which are too bulky to be suitable for POCT diagnosis (Abriola et al., 1999; Soldat et al., 2009). In this study, a bundle of 64 optic fibers connecting with 64-well TEM-microplate are extremely tighten to smartphone camera, which successfully avoid to the uneven imaging weakness directly from a camera (Berg et al., 2015). In addition, the smartphone with an in-stored app can automatically process the light signals, calculate NAb inhibition rates and report the final results according to a higher criterion of 30% inhibition (Tan et al., 2020; Khoury et al., 2021).

5. Conclusion

We developed a novel assay of TEMFIS-sVNT basing on sVNT for quantitatively detecting NAb to SARS-CoV-2 in 64-well TEM-microplate. The reaction signals were transmitted through TEM-microwells connecting 64 optical fibers to a portable immunosensing smartphone reader platform with an in-stored app. This assay was performed in specially designed TEM-microplate, which principally advanced over ELISA-sVNT for rapidly measuring the inhibition capacity of NAb to SARS-CoV-2. TEMFIS-sVNT had strongly statistical correlation with ELISA-sVNT and pVNT, and its cost-effective performance could be done during 45 min without operating by living virus, cell culture and special equipment. TEMFIS-sVNT could be accurately point of care testing of NAb level to predict the acquired protective immunity in COVID-19 patients or vaccinees (Ju et al., 2020; Meyer et al., 2020; Klasse, 2014). Additionally, this one-step assay could be potentially used to measure the antibody reactivity in similar purpose for evaluating other infectious disease progression or vaccine efficacy.

CRediT authorship contribution statement

CW, CL, LZ and QF participated in the study design, analysis of data and writing of the manuscript. CW, ZW, BL, PZ, JL and PZ performed the laboratory examination. JL, YF and QF provided key materials. CW, ZW, QF, TL, RC and CL analyzed data and revised the manuscript. All authors read and approved the final version of manuscript.

Declaration of competing interest

The authors declare that they have no competing financial interests or personal relationships that could have appeared to influence the work reported in this paper.

Acknowledgments

The authors thank Shenzhen CDC for providing COVID-19 patients' serum samples, Southern Medical University Nanfang Hospital for providing vaccinees' or patients' blood samples, and Guangzhou, Shenzhen, Harbin, Chengdu and Xi'an Blood Centers for providing healthy blood donor samples.

This work was supported by grants from National Natural Science Foundation of China (No. 32070929), and Guangzhou Bai Rui Kang (BRK) Biological Science and Technology Limited Company.

Appendix A. Supplementary data

Supplementary data to this article can be found online at https://doi.org/10.1016/j.bios.2021.113550.

References

Abe, K.T., Li, Z., Samson, R., Samavarchi-Tehrani, P., Valcourt, E.J., Wood, H., Budylowski, P., Dupuis, A.P., Girardin, R.C., Rathod, B., Wang, J.H., Barrios-Rodiles, M., Colwill, K., McGeer, A.J., Mubareka, S., Gommerman, J.L., Durocher, Y.,

Ostrowski, M., McDonough, K.A., Drebot, M.A., Drews, S.J., Rini, J.M., Gingras, A.C., 2020. JCI Insight 5, 1–14.
Abriola, L., Chin, M., Fuerst, P., Schweitzer, R., Sills, M.A., 1999. J. Biomol. Screen 4, 121–127.
Barnes, C.O., West, A.P., Huey-Tubman, K.E., Hoffmann, M.A.G., Sharaf, N.G., Hoffman, P.R., Koranda, N., Gristick, H.B., Gaebler, C., Muecksch, F., Lorenzi, J.C.C., Finkin, S., Hägglöf, T., Hurley, A., Millard, K.G., Weisblum, Y., Schmidt, F., Hatziioannou, T., Bieniasz, P.D., Caskey, M., Robbiani, D.F., Nussenzweig, M.C., Bjorkman, P.J., 2020. Cell 182, 828–842 e16.
Berg, B., Cortazar, B., Tseng, D., Ozkan, H., Feng, S., Wei, Q., Yan-lok, R., Burbano, J., Farooqui, Q., Lewinski, M., Carlo, D., Di, Garner, O.B., Ozcan, A., Names, A., Berg, B., Cortazar, B., Tseng, D., Ozkan, H., Feng, S., Wei, Q., Chan, R.Y., Burbano, J., Lewinski, M., Carlo, D., Di, Garner, O.B., 2015. ACS Nano 9, 7857.
Chan, J.F.W., Kok, K.H., Zhu, Z., Chu, H., To, K.K.W., Yuan, S., Yuen, K.Y., 2020. Emerg. Microb. Infect. 9, 221–236.
Chen, Y., Liu, Q., Guo, D., 2020. J. Med. Virol. 92, 418–423.
Gorbalenya, A.E., Baker, S.C., Baric, R.S., de Groot, R.J., Drosten, C., Gulyaeva, A.A., Haagmans, B.L., Lauber, C., Leontovich, A.M., Neuman, B.W., Penzar, D., Perlman, S., Poon, L.L.M., Samborskiy, D.V., Sidorov, I.A., Sola, I., Ziebuhr, J., 2020. Nat. Microbiol. 5, 536–544.
Hu, J., Gao, Q., He, C., Huang, A., Wang, K., 2020. Genes Dis 7, 551–557.
Jokerst, J.V., Floriano, P.N., Christodoulides, N., Simmons, G.W., McDevitt, J.T., 2008. Lab Chip 8, 2079–2090.
Ju, B., Zhang, Q., Ge, J., Wang, R., Sun, J., Ge, X., Yu, Jiazhen, Shan, S., Zhou, B., Song, S., Tang, X., Yu, Jinfang, Lan, J., Yuan, J., Wang, H., Zhao, Juanjuan, Zhang, S., Wang, Y., Shi, X., Liu, L., Zhao, Jincun, Wang, X., Zhang, Z., Zhang, L., 2020. Nature 584, 115–119.
Khoury, D.S., Cromer, D., Reynaldi, A., Schlub, T.E., Wheatley, A.K., Juno, J.A., Subbarao, K., Kent, S.J., Triccas, J.A., Davenport, M.P., 2021. Nat. Med. 27, 1205–1211.
Klasse, P.J., 2014. Adv. Biol. 2014 1–24.
Lan, J., Ge, J., Yu, J., Shan, S., Zhou, H., Fan, S., Zhang, Q., Shi, X., Wang, Q., Zhang, L., Wang, X., 2020. Nature 581, 215–220.
Li, Fang, 2016. Annu. Rev. Virol. 3, 1954–1964.
Li, Q., Guan, X., Wu, P., Wang, X., Zhou, L., Tong, Y., Ren, R., Leung, K.S.M., Lau, E.H.Y., Wong, J.Y., Xing, X., Xiang, N., Wu, Y., Li, C., Chen, Q., Li, D., Liu, T., Zhao, J., Liu, M., Tu, W., Chen, C., Jin, L., Yang, R., Wang, Q., Zhou, S., Wang, R., Liu, H., Luo, Y., Liu, Y., Shao, G., Li, H., Tao, Z., Yang, Y., Deng, Z., Liu, B., Ma, Z., Zhang, Y., Shi, G., Lam, T.T.Y., Wu, J.T., Gao, G.F., Cowling, B.J., Yang, B., Leung, G.M., Feng, Z., 2020. N. Engl. J. Med. 382, 1199–1207.
Luo, S., Zhang, P., Ma, X., Wang, Q., Lu, J., Liu, B., Zhao, W., Allain, J.P., Li, C., Li, T., 2019. Virus Res. 268, 1–10.
Luo, S., Zhao, W., Ma, X., Zhang, P., Liu, B., Zhang, L., Wang, W., Wang, Y., Fu, Y., Allain, J.P., Li, T., Li, C., 2020. PLoS Neglected Trop. Dis. 14, 1–20.
Luo, S., Zhang, P., Liu, B., Yang, C., Liang, C., Wang, Q., Zhang, L., Tang, X., Li, J., Hou, S., Zeng, J., Fu, Y., Allain, J.-P., Li, T., Zhang, Y., Li, C., 2021. Emerg. Microb. Infect. 10, 1002–1015.
Mendoza, E.J., Manguiat, K., Wood, H., Drebot, M., 2020. Curr. Protoc. Microbiol. 57, 1–15.
Meyer, B., Reimerink, J., Torriani, G., Brouwer, F., Godeke, G.J., Yerly, S., Hoogerwerf, M., Vuilleumier, N., Kaiser, L., Eckerle, I., Reusken, C., 2020. Emerg. Microb. Infect. 9, 2394–2403.
Nie, J., Li, Q., Wu, J., Zhao, C., Hao, H., Liu, H., Zhang, L., Nie, L., Qin, H., Wang, M., Lu, Q., Li, X., Sun, Q., Liu, J., Fan, C., Huang, W., Xu, M., Wang, Y., 2020. Nat. Protoc. 15, 3699–3715.
Passariello, M., Gentile, C., Ferrucci, V., Sasso, E., Vetrei, C., Fusco, G., Viscardi, M., Brandi, S., Cerino, P., Zambrano, N., Zollo, M., De Lorenzo, C., 2021. Sci. Rep. 11, 11046.
Ren, L., Li, C., Yang, Y., 2020. Infect. Genet. Evol. 82, 104285.
Rodriguez, W.R., Christodoulides, N., Floriano, P.N., Graham, S., Mohanty, S., Dixon, M., Hsiang, M., Peter, T., Zavahir, S., Thior, I., Romanovicz, D., Bernard, B., Goodey, A. P., Walker, B.D., McDevitt, J.T., 2005. PLoS Med. 2, 0663–0672.
Shi, R., Shan, C., Duan, X., Chen, Z., Liu, P., Song, J., Song, T., Bi, X., Han, C., Wu, L., Gao, G., Hu, X., Zhang, Y., Tong, Z., Huang, W., Liu, W.J., Wu, G., Zhang, B., Wang, L., Qi, J., Feng, H., Wang, F.S., Wang, Q., Gao, G.F., Yuan, Z., Yan, J., 2020. Nature 584, 120–124.
Soldat, D.J., Barak, P., Lepore, B.J., 2009. J. Chem. Educ. 86, 617–620.
Tan, C.W., Chia, W.N., Qin, X., Liu, P., Chen, M.I.C., Tiu, C., Hu, Z., Chen, V.C.W., Young, B.E., Sia, W.R., Tan, Y.J., Foo, R., Yi, Y., Lye, D.C., Anderson, D.E., Wang, L. F., 2020. Nat. Biotechnol. 38, 1073–1078.
Tian, S., Zhang, W., Shi, J., Guo, Z., Li, M., 2020. Anal. Sci. 36, 953–957.
Walls, A.C., Park, Y.J., Tortorici, M.A., Wall, A., McGuire, A.T., Veesler, D., 2020. Cell 181, 281–292 e6.
Wang, C., Wang, L., Zhu, X., Wang, Y., Xue, J., 2012. Lab Chip 12, 1710–1716.
Wu, A., Peng, Y., Huang, B., Ding, X., Wang, X., Niu, P., Meng, J., Zhu, Z., Zhang, Z., Wang, J., Sheng, J., Quan, L., Xia, Z., Tan, W., Cheng, G., Jiang, T., 2020. Cell Host Microbe 27, 325–328.
Zhou, Y., Yang, Y., Huang, J., Jiang, S., Du, L., 2019. Viruses 11, 1–18.
Zhou, P., Yang, X., Lou, Wang, X.G., Hu, B., Zhang, L., Zhang, W., Si, H.R., Zhu, Y., Li, B., Huang, C.L., Chen, H.D., Chen, J., Luo, Y., Guo, H., Jiang, R., Di, Liu, M.Q., Chen, Y., Shen, X.R., Wang, X., Zheng, X.S., Zhao, K., Chen, Q.J., Deng, F., Liu, L.L., Yan, B., Zhan, F.X., Wang, Y.Y., Xiao, G.F., Shi, Z.L., 2020. Nature 579, 270–273.